Article

Role of Mechanochemistry in Solid Form Selection and Identification of the Drug Praziquantel

Basanta Saikia,* Andreas Seidel-Morgenstern, and Heike Lorenz

Read Online

ACCESS | Metrics & More | Article Recommendations | SI Supporting Information

ABSTRACT: Identification of all possible polymorphs for a pharmaceutical compound is vital for the better formulation of medicine with desired properties. This study demonstrates the application of a mechanochemical approach to reveal new polymorphs of a drug and the potential of variable amounts of solvent in liquid-assisted grinding for solid form screening. Without solvent and by varying the amount of solvent added, we found two new polymorphs and an amorphous form, which were not reported previously. The finding portrays the advantage of the mechanochemical approach as a means of the polymorph screening strategy. While the focus here was on praziquantel, a similar approach is applicable to other pharmaceutical systems. This study also contributed to reinvestigate the solid-state behavior of the chiral praziquantel system, including the melt phase diagram and the role of experimental conditions on its phase behavior.
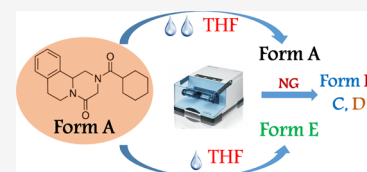
1. INTRODUCTION

Polymorphism is very significant for crystalline materials and can be defined as the ability of a compound to exhibit more than one crystalline form.[1,2] A better understanding of polymorphism is vital for the pharmaceutical industry, as most of the drug molecules are prone to be polymorphic.[3] Moreover, different polymorphs of a drug molecule can have completely different physiochemical properties such as solubility, permeability, stability, tablettability, hygroscopicity, and so on, properties that are crucial in pharmaceutical formulation development.[4] Thus, screening for all the possible polymorphic forms of a drug and control of the polymorphic form of drug molecules is of considerable importance.[5−7] In recent years polymorph screening through mechanochemistry is becoming popular as a greener approach.[8,9] Furthermore, liquid-assisted grinding (LAG) is one of the frequently employed strategies for mechanochemical control over cocrystal, polymorphs, etc.[9−11] The stabilization of a specific polymorph of γ-aminobutyric acid by using the LAG technique with high-polarity solvents has been reported recently.[12] Emmerling and co-workers demonstrated the formation of a metastable form III of benzamidine by using nicotinamide seeds in a LAG experiment with ethanol.[13] There is very limited study on the application of variable amounts of solvent in liquid-assisted grinding (VALAG) on solid form screening and control.[9] Jones and co-workers demonstrated the applicability of VALAG to explore polymorph diversity of the caffeine—anthranilic acid cocrystal system.[8] A thorough explanation of VALAG remains challenging; Belenguer et al. described that a change in the amount of a liquid during grinding would affect the particle size of the grinded material and thus influence the relative stability of the polymorphic forms.[14,15]

The experimental conditions affect the polymorphic outcome for a molecule; thus, understanding and controlling the experimental parameters to control the polymorphic behavior is of high scientific and industrial concern.[6,7] In this study, mechanochemistry was used to investigate the solid-state forms of racemic praziquantel (PRA) (Scheme 1). It is a chiral

Scheme 1. Molecular Structure of the Drug Praziquantel
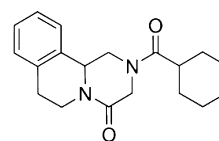
prescribed drug for the treatment of schistosomiasis worms.[16] A background survey of PRA reveals that it has three reported polymorphs, several cocrystals, and also hydrates.[17−21] The marketed form A is a racemic compound with a triclinic crystal structure (CSD refcode-TELCEU).[18] It has a disordered structure with two out of four molecules that are disordered in the asymmetric unit, the carbonyl groups have syn conformation.[22] Zanolla et al. recently reported two anhydrate polymorphic forms, i.e., form B (CSD refcode-TELCEU01)[18] and form C (CSD refcode-GOYZOM),[23] that are produced via neat grinding of the commercial form A of PRA for about 4 h in a vibrational mixer mill. A racemic hemihydrate form[17] of

PRA obtained through mechanochemistry is also depicted by this group and a monohydrate form by Salazar-Rojas et al.[20]

In this study, we are particularly interested in the role of mechanochemistry in solid form selection and identification of PRA, particularly investigating the polymorphism of PRA by using the VALAG technique. We identified and investigated a new polymorphic anhydrous crystalline form of PRA (designated as form D) from neat grinding. Furthermore, a new polymorphic form E and a pure amorphous form (designated as form F) have been obtained by using the VALAG technique. The materials were characterized by differential scanning calorimetry (DSC) and powder X-ray diffraction (PXRD), combined with attenuated total reflectance-Fourier transform infrared spectroscopy (ATR-FTIR) and FT-Raman spectroscopy.

Understanding the solid-state phase behavior of a chiral compound is also very important, as it directs the way for resolution via crystallization. We have exploited mechanochemistry as a tool to study the phase behavior of PRA. The phase diagrams (melt and solubility) of PRA have been reported earlier in different studies, but the results are uneven and showed the uncertain nature of PRA.[24−26] In this work, we try to look at the solid-state behavior of PRA by varying the different experimental conditions. Thermal properties are useful in classifying the type of racemic mixture.[27,28] In this regard, three types of solid-state phases may appear from an enantiomeric 1:1 mixture, i.e., a racemic compound, a conglomerate, and a solid solution.[29,30] Furthermore, chiral systems forming solid solutions at a racemic composition are classified into three categories, i.e., I, an ideal solid solution, where the solid solution has the same melting point as the enantiomer, and II and III, solid solutions showing a maximum or minimum melting point at the racemic composition, respectively.[29] The behavior of a chiral material to form both a racemic compound and a solid solution system is reported to occur rather rarely.[31] This study found that although PRA typically forms a racemic compound, however, it forms partial solid solutions (type II) in liquid-assisted mechanochemical grinding up to a composition of approximately 75% of R-PRA.

2. EXPERIMENTAL SECTION

2.1. Materials. Rac-praziquantel (PRA) and R-praziquantel (R-PRA) were received from Merck Deutschland GmbH and were used without further purification. Millipore water from a Milli-Q system (Merck Millipore, Milli-Q Advantage) and HPLC-grade solvents were used for crystallization experiments.

2.2. Analytical Instruments. The solid-state properties of the system were investigated by PXRD analysis with an X'pert Pro diffractometer (PANalytical GmbH, Kassel, Germany) with Cu Kα radiation and an X'Celerator detector in the 2θ range of 3–40° with a step size of 0.017° and a step time of 50 s. Temperature-resolved powder X-ray diffraction (TR-PXRD) was performed in the 2θ range of 3°–30° with a step size of 0.017°. Thermal analysis was carried out using a DSC 131 (Setaram, Diepholz, Germany), which was regularly calibrated using highly pure standard materials. HPLC analyses were performed to check the enantiomeric composition of the material. An Agilent 1200 system (Agilent Technologies, Waldbronn, Germany) equipped with a Chiralcel OD-H column (0.46 × 25 cm, Chiral Technologies Europe, Illkirch, France) was used with the following conditions: temperature 23 °C, eluent mixture: 60: (v/v), n-heptane, ethanol, and diethanolamine, flow rate: 1.0 mL/min, and UV wavelength: 265 nm. FT-IR spectra were collected at the solid-state using a spectrophotometer Bruker ALPHA II (Bruker, Karlsruhe, Germany). The analyzed range of wavenumbers was from 600 to 4000 cm⁻¹, with a scan number of 4. Raman spectra were collected at

the solid-state using an FT-Raman spectrometer Bruker MultiRAM (Bruker, Karlsruhe, Germany). Solid-state NMR measurement was acquired by using an NMR BRUKER Avance 300 MHz WB spectrometer (Bruker, Karlsruhe, Germany). ^{13}C CPMAS spectra were measured at a spinning speed of 5 kHz with a RAMP-CP pulse sequence (pulse of 3.2 μs; contact time of 2 ms) and a recycle time of 38 s and 280 scans.

2.3. Mechanochemical Grinding Procedures. The mechanochemical grinding experiments were performed by using an MM400 vibrational mill (Retsch, Haan, Germany) at 25 Hz for variable time periods. PRA form D was obtained from neat grinding. PRA form A (250 mg) was added to a 10 mL zirconium oxide jar equipped with two zirconia balls (diameter of 7 mm) and neat grinded for 4 h; the samples were kept overnight in a desiccator. The product was examined by DSC, PXRD, FT-IR, and FT-Raman spectroscopy. Subsequently, the material was further ground for another 1 h. The obtained material was again subjected to different analyses. The conversion of PRA form A into PRA form D was eventually assessed by PXRD, DSC, and FT-IR.

For LAG experiments an equal amount of material (250 mg) was added to a 10 mL zirconium oxide jar equipped with two zirconia balls (diameter of 7 mm). The amounts of solid were kept fixed for each solvent-assisted mechanochemical grinding experiment, the amount of the liquid added was varied and volumes ranged 10−30 μL. The lid of the ball mill jar was closed immediately to avoid evaporation of the solvent. The samples were milled for different time periods, and the ground samples were analyzed by DSC, PXRD, and FT-IR to determine the solid-state form.

2.4. Solution Crystallization of Praziquantel. Slow evaporation was employed for the crystallization of PRA from different solvents. Around 50 mg of PRA was taken in vials and dissolved by adding 2 mL of different solvents (see Table 2). The vials were left at room temperature in a desiccator for slow evaporation. The retrieved crystals were analyzed by DSC and PXRD.

2.5. Binary Melt Phase Diagram. Different amounts of R- and rac-PRA were weighted to prepare samples (approximately 50 mg) of specific compositions. These mixtures were taken in vials, completely dissolved by adding a sufficient amount of acetone, and afterward kept for recrystallization by slow evaporation at room temperature. Retrieved samples are characterized by DSC and PXRD.

Furthermore, samples for phase diagram studies were prepared by mechanochemical grinding, in particular, to study the solid solution behavior of the PRA system. Therefore, differently composed mixtures of R- and rac-PRA (approximately 50 mg) were ground in a mortar and pestle for at least 20 min by dropwise addition of acetone. In a separate batch, samples of different compositions were prepared by neat grinding for 20 min by using a mortar and pestle. All the materials were subjected to PXRD and DSC analysis.

The DSC measurements were carried out with a constant heating rate of 2 K/min in the range from 25 to 150 °C, under a pure helium atmosphere at 8 mL/min. Eutectic and pure compound melting temperatures were taken from the corresponding peak onsets, liquidus temperatures for mixtures from the peak maximum, and solid solution related solidus and liquidus data from starting of the melting peak and peak maximum, respectively. The Schröder−Van Laar (1) and Prigogine−Defay (2) equations have been used to predict the solid−liquid equilibria in ideal binary systems at temperature T_f.[32]

$$\ln x = \frac{\Delta H_A^f}{R}\left(\frac{1}{T_A^f} - \frac{1}{T_f}\right)$$

(1)

$$\ln 4x(1-x) = \frac{2\Delta H_R^f}{R}\left(\frac{1}{T_R^f} - \frac{1}{T_f}\right)$$

(2)

In these equation x represents the mole fraction of the enantiomer in the mixture, R is the gas constant, T_A^f and T_R^f the melting temperature of the enantiomer and racemate, and ΔH_A^f and ΔH_R^f the enthalpy of fusion of the enantiomer and racemate, respectively.

3. RESULTS AND DISCUSSION

3.1. Polymorphic Outcome from Neat Grinding.
Polymorph screening of PRA has been done via mechanochemical neat grinding. Definite amounts of PRA were grinded in a ball mill and the retrieved samples were examined at definite time intervals by DSC, FT-IR, and PXRD. The results of the DSC analyses for the ground materials collected at different time intervals are presented in Figure 1. Polymorph A,
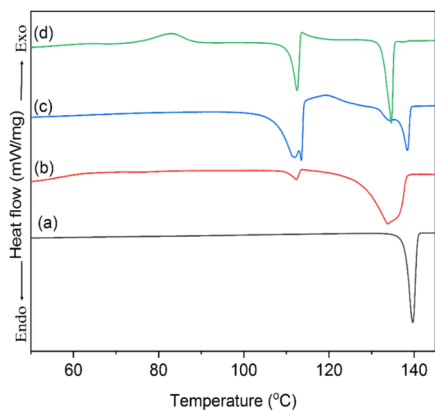

Figure 1. DSC thermograms of a PRA sample ground for various time intervals up to 5 h; (a) initial form A, (b) 1.5 h grinding, (c) 4 h grinding, and (d) 5 h grinding.

the commercial form, has a melting point of 139.6 °C (Figure 1a), while polymorphs B and C have a melting onset of 112.0 and 110.2 °C, respectively. The DSC profile of the sample ground for 4 h (Figure 1c) shows four significant endothermal peaks, whereas those at 110.2, 112.0, and 139.2 °C can be assigned to the reported PRA polymorphs C, B, and A, respectively. The peak (or "shoulder") appearing at 133.3 °C indicates a possible new solid-state form. Subsequent grinding of this material for a further hour and studied by DSC analysis (Figure 4d) reveals that the endothermic peak at 110.2 °C (i.e.,

polymorph C) is vanished entirely along with a considerable decrease of the polymorph A peak. Interestingly, an exothermic peak observed for this sample at ∼85 °C indicates the possible partial amorphization and respective recrystallization of the ground sample. To interpret the observed phase transitions with temperature, a sample obtained after 5 h of grinding was studied by TR-PXRD at 30, 60, 85, 100, and 125 °C, after keeping the samples for 2 min at each of those temperatures, and followed by cooling them back to room temperature. The obtained results are shown in Figure 2a.

The intensity of the PXRD patterns at 30 and 60 °C is relatively low suggesting a mixture of amorphous and crystalline material. The intensities of the peaks increased substantially at 85 and 100 °C accompanied by some additional peaks. A complete transformation is detected at 125 °C showing an entirely new powder pattern different from those of the already reported polymorphs A, B, and C (see also Figure 2b), which suggests the occurrence of a new form of PRA. For this new polymorph, designated form D in the following study, new characteristic peaks appeared at 2θ = 3.3°, 7.8°, 9.4°, 11.4°, and 15.0°, which was connected with the disappearance of characteristic peaks of polymorph B at 2θ = 6.7°, 8.4°, 15.7°, and 20.3°. Consequently, the DSC profile for the 5 h ground sample (Figure 1d) can be interpreted as follows: first, partial recrystallization of form B at ∼85 °C followed by its melting at 112 °C; directly from the melt, new form D crystallizes and melts at 133.3 °C. Also, a small residue of high-temperature stable form A can be detected in DSC and PXRD patterns as well.

Different molecular packings of the PRA polymorphs are further identified by FT-IR. The respective FT-IR spectrum of PRA form D compared to forms A and B is shown in Figure 3. The FT-IR pattern obtained for the new D-form differs from those of polymorphs A and B.[22] The C=O stretching frequency for form D is observed at 1645 cm^{-1}, which is shifted by about 4 cm^{-1} in comparison to form A (1649 cm^{-1}) and form B (1641 cm^{-1}). The signal at 758 cm^{-1} corresponds to the bending vibration of the aromatic −CH of PRA. Significant shifting is also observed in aliphatic −CH stretching for the polymorph D. The different −C=O stretching frequencies of carbonyl groups is a further validation of
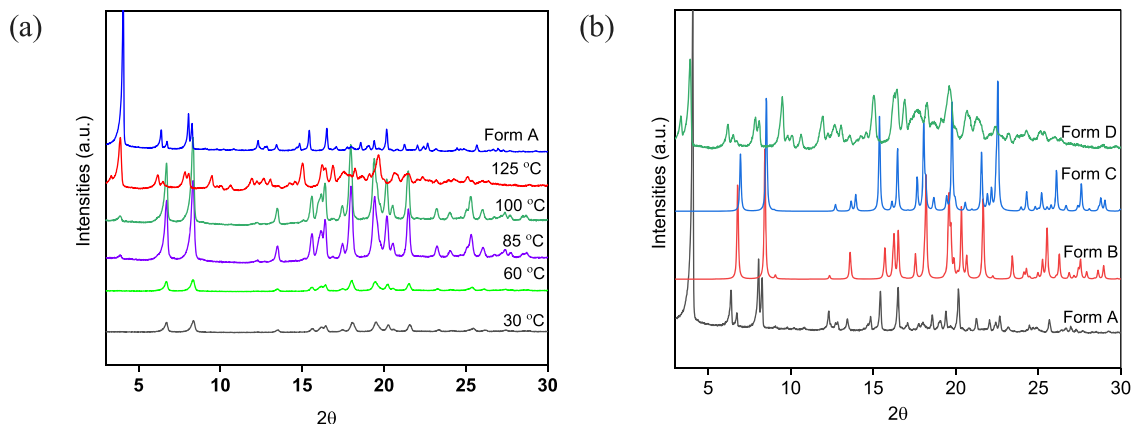

Figure 2. (a) PXRD patterns obtained at various temperatures for a PRA sample ground for 5 h and comparison with form A. (b) Comparison of the PXRD pattern of A and the calculated PXRD patterns of forms B and C[18,23] retrieved from the CCDC database with the new form D. The PXRD pattern of PRA form D is different from the already known PRA forms A, B, and C; characteristic reflections of PRA form D were found at 2θ = 3.3°, 7.8°, 9.4°, 11.4°, and 15°.
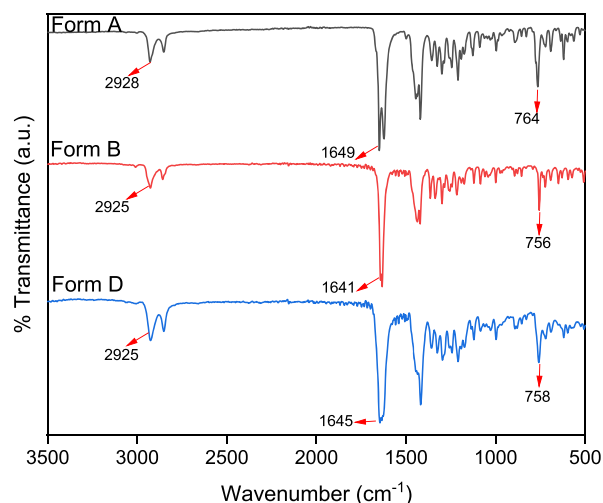
Figure 3. FT-IR spectra comparison of PRA forms A, B, and D. Significant differences are observed, e.g., in C=O stretching frequencies for the polymorphs, and are indicated by arrows.

various crystal packings and thereby the presence of the new polymorph D of PRA.

To identify the phase stability and possible transformation of the PRA phases, the material obtained from 5 h grinding was further subjected to recrystallization from acetone and a slurry in acetone was also prepared. The materials obtained from the slurry experiment and the recrystallized products from solvent evaporation were analyzed by DSC, FT-IR, and PXRD analysis. The materials are found to be transformed to the original form A, exemplarily shown for PXRD patterns in Figure 4 (also verifying that no chemical changes occurred
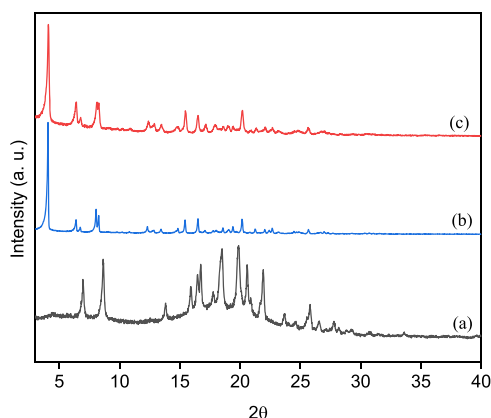

Figure 4. Comparison of PXRD patterns of (a) sample of PRA ground for 5 h, (b) recrystallized product of the ground sample from acetone, and (c) form A of PRA.

during grinding experiments). The conversion to the original form A is additionally confirmed by FT-IR. To further prove that no degradation of the material occurred on intensive grinding, the ground materials were subjected to HPLC analysis, which did not give any indication of other components present other than PRA. TR-PXRD analysis of the starting material has been performed to see if there is any transformation or thermal degradation of PRA form A. No significant changes have been observed in PXRD patterns (see Supporting Information Figure S1), which suggests the thermal phase stability of polymorph A up to 135 °C.

3.2. Effect of the Variable Amount of Liquid on Grinding Results.

Solution crystallization of PRA always resulted in form A in more than 10 solvents (see Table 2 below). To understand the role of solvent in mechanochemistry for solid form selection of PRA, LAG has been performed by considering different laboratory solvents. Therefore, always a fixed amount of PRA (250 mg) was used but the solvent and the solvents' volume were varied.

Supporting Information Figure S2 shows the DSC curves of 1 h LAG of PRA in the presence of 5, 10, 20, and 30 μL of THF. LAG with 5 μL of THF resulted in a mixture of form C with a minute amount of A. A significant change in melting behavior was observed for the material obtained from LAG with 10 μL of THF. The results of the DSC analyses for the materials obtained from LAG with the addition of THF in comparison to unground PRA are shown in Figure 5. The peak
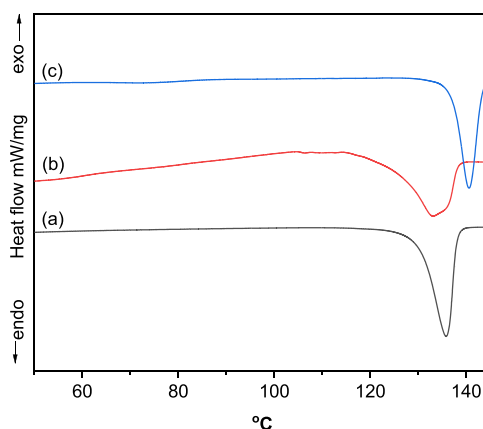

Figure 5. DSC thermograms of PRA (c) and the samples obtained from solvent-assisted grinding (10 μL of THF) for 1 h (a) and 2 h (b).

in DSC curve (a) appearing at 135.5 °C indicates a possible new solid form designated as E. Further grinding of E for another 1 h (curve (b) in Figure 5) produced a partially amorphous material and shows a broad exotherm in the DSC curve. The PXRD pattern of form E is compared with the diffraction pattern of PRA form A in Figure 6. The two patterns exhibit differences in the 2θ range of 5°−30°. The characteristic diffraction peak for polymorph A at 6.7° disappeared and a new peak appeared at 21.8°. Furthermore, there are significant changes in the intensity of the diffraction
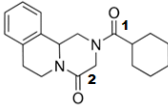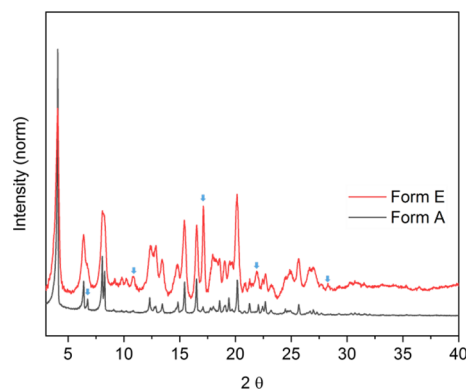

Figure 6. PXRD pattern comparison of PRA form A and new form E. Arrows indicate characteristic peaks.

peaks observed at $2\theta = 9.8°$, $10.1°$, $10.9°$, and $17.1°$. Despite several attempts, we failed to obtain a single crystal for the material, as upon solution crystallization the samples transformed to the original form A. To further support the findings we performed solid-state NMR and FT-Raman spectroscopy.

The ^{13}C CPMAS SS-NMR carbonyl chemical shift for PRA form E is compared with the carbonyl shifts for reported polymorphic forms A, B, and C in Table 1. The NMR

Table 1. Carbonyl Group Chemical Shift Analysis for the ^{13}C SS-NMR Spectra of PRA Form E, Compared with the Reported Forms A, B, and C, from Refs 17, 18

Polymorph	C=O (1)	C=O (2)	
A	175.4, 176.2	165.8, 164.6, 162.1	
B	173.6	164.3	
C	173.3	165.4	
E	175.3, 173.0	162.2	Praziquantel

spectrum of form E itself is presented in Suppoting Information Figure S3. The analysis data verify the formation of a new pure phase, i.e., form E, different from the reported polymorphs.[17] FT-Raman spectra comparison also supports the formation of a new polymorphic form (see Suppoting Information Figure S4).

The results demonstrate the applicability of polymorph screening via the VALAG technique simply by varying the amount of the same solvent. It is noteworthy that the addition of only 10 μL of THF or acetone has a significant effect on the polymorphic outcome of PRA (see Table 2). Neat grinding for

Table 2. Comparison of PRA Polymorph Screening Results Obtained by Using Solution Crystallization and LAG in the Presence of Different Volumes of Solvent (VALAG)

sl. no.	solvent	solution crystallization	VALAG (1 h) 30 μL	VALAG (1 h) 10 μL
1	ethanol	A	A	A
2	methanol	A	A	A
3	1-butanol	A	A	A
4	1-propanol	A	A	A
5	nitromethane	A	A	A
6	ethyl acetate	A	A	A
7	1,4-dioxane	A	A	A
8	THF	A	A	E
9	acetonitrile	A	A	A
10	acetone	A	A	E
11	toluene	A	A	
12	CHCl$_3$	A	A	A

1 h produced a mixture of forms B and C and the amorphous form (Suppoting Information Figure S8), while LAG with 10 μL of THF or acetone produced the new form E (Table 2). By contrast, LAG with a larger amount of solvent (30 μL and more) does not alter the polymorphic outcome and only produced form A (e.g., Suppoting Information Figure S2) on grinding up to 2 h. Thus, PRA polymorphism depends on the amount of solvent used for the grinding experiment. Volumes of 20 or 30 μL always generated Form A for the same duration (i.e., 1 h) of grinding, while the lower volume, i.e., 10 μL, resulted in form E. Moreover, some solvents did not alter the polymorphic forms on mechanochemical grinding for up to 1 h

irrespective of the amount of solvent added as given in Table 2. For example, acetonitrile, nitromethane, and ethanol for all volumes were selective to one polymorph providing only the form A.

A summary of the VALAG results using THF as solvent is illustrated in Scheme 2. The PXRD pattern of the material

Scheme 2. Schematic Representation of Results of Grinding Experiments with PRA at Different Amounts of THF in Liquid-Assisted Grinding (VALAG)
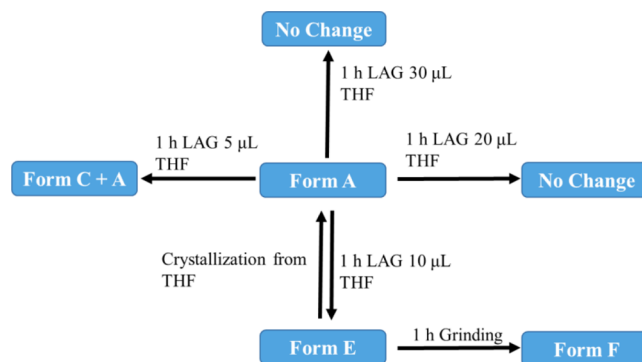
obtained from subsequent 1 h grinding of form E (compare Figure 5, curve (b)) does not show sharp Bragg peaks but a broad halo (Figure 7, 30 °C pattern), thus confirming the
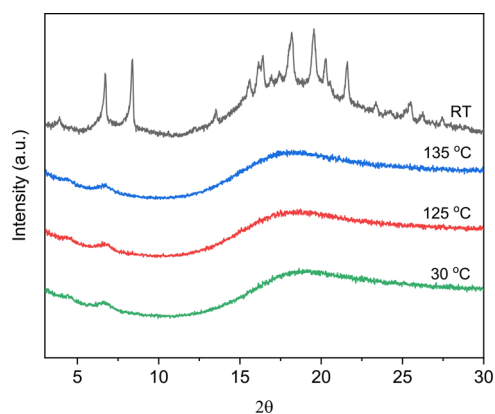

Figure 7. PXRD patterns were obtained at various temperatures for the 2 h LAG sample of PRA with the addition of 10 μL of THF. Upon cooling to RT, the material exhibited partial transformation to polymorph B.

formation of the amorphization product (further designated as F). The results demonstrated that the amorphization of PRA upon milling increases with the addition of a catalytic amount of THF. Note that polymorph D was never observed under the VALAG conditions used. To investigate the stability of the amorphous form, the material was kept at ambient conditions for 2 weeks. PXRD and DSC patterns did not show significant changes. TR-PXRD at 30, 125, and 135 °C still confirmed the amorphous state of the sample (Figure 7). However, after cooling to room temperature (RT), partial transformation to polymorph B was revealed.

Through introducing a trace amount of solvents during milling, polymorph selectivity is achieved for praziquantel polymorphs, which otherwise cannot be produced by solution crystallization or neat grinding under the conditions used. The mechanism why the VALAG technique can provide different
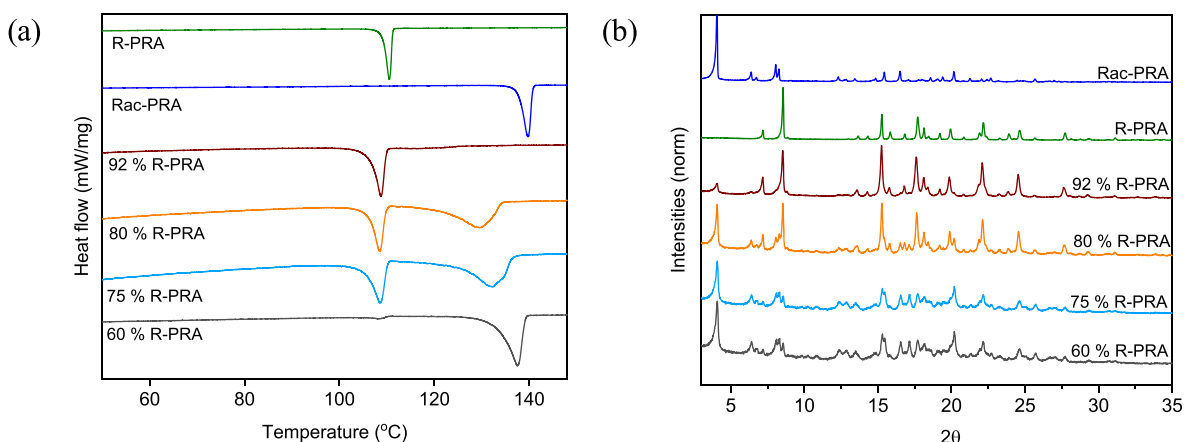
Figure 8. Comparison of DSC profiles (a) and PXRD patterns (b) of samples with different *rac*-PRA/*R*-PRA compositions prepared by neat grinding.
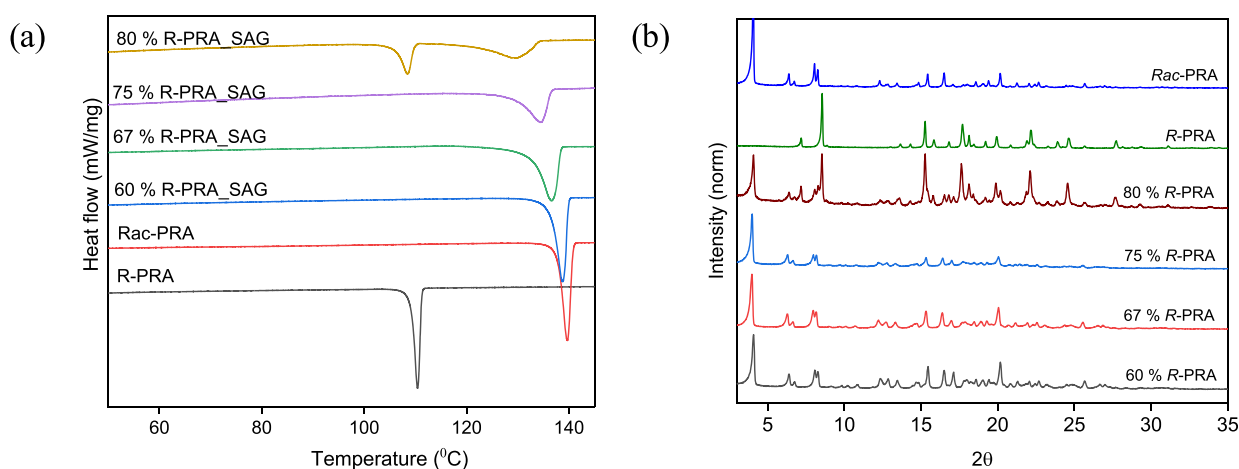

Figure 9. Comparison of DSC profiles (a) and PXRD patterns (b) of samples with different *rac*-PRA/*R*-PRA compositions obtained from LAG.

solid-state forms, though it uses the same liquid, is not readily understood until now. The less amount of solvent could introduce local supersaturation,[33] which can further act as a "seed" to provide a nucleation surface for different polymorphs under specific milling conditions. Moreover, during milling, the particle size of the material decreases and the surface effect becomes more prominent.[14] When adding a trace amount of solvent during grinding, the solvent could interact with the crystal surface via adsorption or solvation effects.[14] If the interaction between the solvent and the surface of the material is very strong, one conformation could be more preferred and accordingly one could expect the retention of a particular conformational polymorph.[22]

3.3. Melt Phase Diagram of Chiral Praziquantel. DSC profiles (Figure 8a) demonstrate the melting behavior of solid samples at different enantiomeric compositions obtained by neat grinding. The DSC curves show melting profiles, consisting of two endothermic peaks corresponding to eutectic melting and the subsequent dissolution effect of the excess racemic compound. The eutectic temperature was found on average at 106.4 °C. The melting point of the racemate (139.6 °C) is significantly higher than that of the enantiomers (110.4 °C) with a melting enthalpy of 96.0 and 69.7 J/g, respectively. Thus, the phase behavior confirms the presence of a eutectic melting at different compositions than the racemic, suggesting praziquantel behaves as a racemic compound-forming system,

which is in good agreement with literature data.[26] The PXRD patterns of the respective samples shown in Figure 8b verify the different structures of *rac*-PRA and its *R*-enantiomer as well as the presence of "mechanical" mixtures of *rac*-PRA (form A) and *R*-PRA in the binary system. The melting data determined are included in the melt phase diagram of the chiral PRA system in Figure 10, marked as liquidus and eutectic (solidus) data from the neat grinded (NG) samples.

In contrast to the behavior of the NG material, samples obtained from liquid-assisted mechanochemical grinding exhibited solid solution behavior up to ~75 wt % enantiomeric composition (Figure 9). The related DSC profiles and PXRD patterns are shown in Figure 9a,b, respectively. PXRD analysis of the samples up to 75 wt % enantiomeric composition show nearly identical diffraction patterns with *rac*-PRA, indicating a solid solution behavior, thus integration of *R*-PRA molecules into the lattice of the racemate. DSC curves of the respective samples obtained by LAG as well as by recrystallization from acetone do not reveal any eutectic melting up to 75 wt % of *R*-PRA in the mixtures but melting peak broadening according to the presence of solid solutions. The corresponding solidus and liquidus temperatures are also integrated into the phase diagram (Figure 10, marked by open and closed circles). At 80 wt % *R*-PRA, i.e., beyond 75 wt % content, eutectic melting is again observed forming the boundary of solid solutions and eutectic behavior in the *rac*-PRA/*R*-PRA system. Consistently,
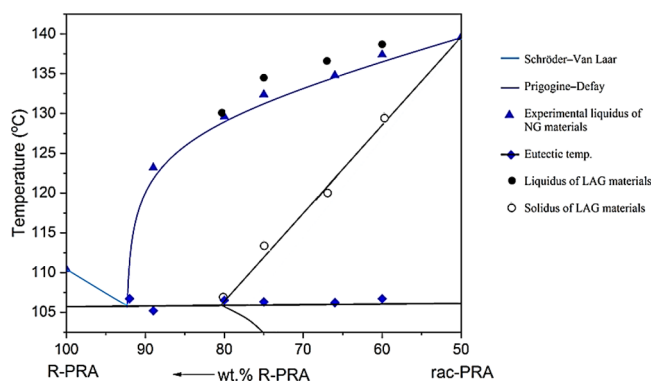
Figure 10. Binary melt phase diagram of the chiral praziquantel system. Only half of the phase diagram, the *R*-PRA/*rac*-PRA side studied, is shown.

the PXRD pattern for this sample confirms the presence of a mechanical mixture, i.e., a two-phase system, consisting of *rac*-PRA (form A) and *R*-PRA. Thus, the results demonstrate again the effect of the process parameters used for preparation on the phase behavior in the PRA system, which, on the other hand, allows systematically altering the phase behavior by varying the experimental conditions.

The phase diagram studies using neat grinding of *rac*-PRA and *R*-PRA always resulted in eutectic behavior; however, solvent-assisted mechanochemical grinding and recrystallization from acetone (results not shown here/see Supporting Information Figure S9) provide solid solutions up to ~75 wt % *R*-PRA composition, which lead to partial miscibility at the solid-state in the PRA system. Beyond ~75 wt %, *R*-PRA content always shows eutectic behavior irrespective of the used experimental conditions. As already mentioned, miscibility at the solid-state is rather rare in chiral systems, in particular full miscibility over the entire composition range. It can be assumed that the liquid-assisted mechanochemical grinding facilitates the faster diffusion of the enantiomer molecules into the racemate lattice, and thereby can provide solid solutions at lower *R*-PRA excesses.

4. CONCLUSIONS

The polymorphic behavior of PRA was investigated by using different techniques such as crystallization from solution, neat grinding and LAG manually, and more intensive machine-supported grinding via mechanochemistry. A new polymorph D of PRA has been identified by neat grinding and characterized by different analytical techniques such as PXRD, DSC, FT-IR, etc. This work highlights the applicability of the VALAG technique as an additional tool for screening the polymorphic behavior of praziquantel. The VALAG technique is effective to generate new polymorph E and an amorphous form of racemic praziquantel (form F). Also, these solid forms were thoroughly characterized by using different analytical techniques. Unfortunately, no suitable single crystals could be grown to describe the crystal structures of forms D and E by single-crystal XRD. In addition, the binary melt phase diagram of the chiral praziquantel system has been reinvestigated. From the results, it was concluded that it is a racemic compound-forming system, which, however, may also show limited miscibility at the solid-state, i.e., formation of partial solid solutions of the racemic compound with the enantiomer. Noteworthy is that the formation of solid solutions or eutectic

mixtures strongly depends on the experimental conditions used. The existence of solid solutions was confirmed up to enantiomeric compositions of ~75% *R*-PRA for the material obtained from liquid-assisted mechanochemical grinding under the conditions used. Overall, this work demonstrated how phase behavior of the same enantiomeric composition can vary based on experimental conditions and confirmed the effectiveness of mechanochemistry for polymorph screening. We have demonstrated that the solid form of an API can also be screened and altered by using the VALAG technique. This work also sought the reconsideration of the traditionally accepted concept "one solvent for one polymorph."[9] A most common technique for polymorph screening by mechanochemistry where only one solvent as the liquid additive is used[8] also needs to be revised. However, the mechanism of how a variable amount of solvent in LAG can provide different solid-state forms is not fully understood and more work is needed to understand solvent effects in the control of the polymorphic behavior of a compound.

■ ASSOCIATED CONTENT

ⓈI Supporting Information

The Supporting Information is available free of charge at https://pubs.acs.org/doi/10.1021/acs.cgd.1c00736.

    PXRD patterns, DSC thermograms, ^{13}C CPMAS spectrum, Raman Spectra, TR-PXRD analysis, DSC pattern, and, comparison of PXRD patterns (PDF)

■ AUTHOR INFORMATION

Corresponding Author

    Basanta Saikia − *Max Planck Institute for Dynamics of Complex Technical Systems, Magdeburg 39106, Germany;* ⓞ orcid.org/0000-0001-6138-9898; Email: bsaikia1@gmail.com, saikia@mpi-magdeburg.mpg.de

Authors

    Andreas Seidel-Morgenstern − *Max Planck Institute for Dynamics of Complex Technical Systems, Magdeburg 39106, Germany;* ⓞ orcid.org/0000-0001-7658-7643

    Heike Lorenz − *Max Planck Institute for Dynamics of Complex Technical Systems, Magdeburg 39106, Germany;* ⓞ orcid.org/0000-0001-7608-0092

Complete contact information is available at:
https://pubs.acs.org/10.1021/acs.cgd.1c00736

■ REFERENCES

(1) Bernstein, J., *Polymorphism in Molecular Crystals* Oxford University Press: 2007.

(2) Cruz-Cabeza, A. J.; Reutzel-Edens, S. M.; Bernstein, J. Facts and fictions about polymorphism. *Chem. Soc. Rev.* **2015**, *44*, 8619−8635.

(3) Cruz-Cabeza, A. J.; Feeder, N.; Davey, R. J. Open questions in organic crystal polymorphism. *Commun. Chem.* **2020**, *3*, 142.

(4) Lee, A. Y.; Erdemir, D.; Myerson, A. S. Crystal Polymorphism in Chemical Process Development. *Annu. Rev. Chem. Biomol. Eng.* **2011**, *2*, 259−280.

(5) Taylor, C. R.; Mulvee, M. T.; Perenyi, D. S.; Probert, M. R.; Day, G. M.; Steed, J. W. Minimizing Polymorphic Risk through Cooperative Computational and Experimental Exploration. *J. Am. Chem. Soc.* **2020**, *142*, 16668−16680.

(6) Bora, P.; Saikia, B.; Sarma, B. Oriented Crystallization on Organic Monolayers to Control Concomitant Polymorphism. *Chem.− Eur. J.* **2020**, *26*, 699−710.

(7) Saikia, B.; Mulvee, M. T.; Torres-Moya, I.; Sarma, B.; Steed, J. W. Drug Mimetic Organogelators for the Control of Concomitant Crystallization of Barbital and Thalidomide. *Cryst. Growth Des.* **2020**, *20*, 7989−7996.

(8) Hasa, D.; Miniussi, E.; Jones, W. Mechanochemical Synthesis of Multicomponent Crystals: One Liquid for One Polymorph? A Myth to Dispel. *Cryst. Growth Des.* **2016**, *16*, 4582−4588.

(9) Hasa, D.; Jones, W. Screening for new pharmaceutical solid forms using mechanochemistry: A practical guide. *Adv. Drug Delivery Rev.* **2017**, *117*, 147−161.

(10) Tan, D.; Loots, L.; Friščić, T. Towards medicinal mechanochemistry: evolution of milling from pharmaceutical solid form screening to the synthesis of active pharmaceutical ingredients (APIs). *Chem. Commun.* **2016**, *52*, 7760−7781.

(11) Sarma, B.; Saikia, B. Hydrogen bond synthon competition in the stabilization of theophylline cocrystals. *CrystEngComm* **2014**, *16*, 4753−4765.

(12) Wang, L.; Sun, G.; Zhang, K.; Yao, M.; Jin, Y.; Zhang, P.; Wu, S.; Gong, J. Green Mechanochemical Strategy for the Discovery and Selective Preparation of Polymorphs of Active Pharmaceutical Ingredient γ-Aminobutyric Acid (GABA). *ACS Sustainable Chem. Eng.* **2020**, *8*, 16781−16790.

(13) Fischer, F.; Greiser, S.; Pfeifer, D.; Jäger, C.; Rademann, K.; Emmerling, F. Mechanochemically Induced Conversion of Crystalline Benzamide Polymorphs by Seeding. *Angew. Chem., Int. Ed. Engl.* **2016**, *55*, 14281−14285.

(14) Belenguer, A. M.; Lampronti, G. I.; De Mitri, N.; Driver, M.; Hunter, C. A.; Sanders, J. K. M. Understanding the Influence of Surface Solvation and Structure on Polymorph Stability: A Combined Mechanochemical and Theoretical Approach. *J. Am. Chem. Soc.* **2018**, *140*, 17051−17059.

(15) Belenguer, A. M.; Lampronti, G. I.; Cruz-Cabeza, A. J.; Hunter, C. A.; Sanders, J. K. M. Solvation and surface effects on polymorph stabilities at the nanoscale. *Chem. Sci.* **2016**, *7*, 6617−6627.

(16) Cioli, D.; Pica-Mattoccia, L. Praziquantel. *Parasitol. Res.* **2003**, *90*, S3−S9.

(17) Zanolla, D.; Hasa, D.; Arhangelskis, M.; Schneider-Rauber, G.; Chierotti, M. R.; Keiser, J.; Voinovich, D.; Jones, W.; Perissutti, B. Mechanochemical Formation of Racemic Praziquantel Hemihydrate with Improved Biopharmaceutical Properties. *Pharmaceutics* **2020**, *12*, 289.

(18) Zanolla, D.; Perissutti, B.; Passerini, N.; Chierotti, M. R.; Hasa, D.; Voinovich, D.; Gigli, L.; Demitri, N.; Geremia, S.; Keiser, J.; Cerreia Vioglio, P.; Albertini, B. A new soluble and bioactive polymorph of praziquantel. *Eur. J. Pharm. Biopharm.* **2018**, *127*, 19−28.

(19) Espinosa-Lara, J. C.; Guzman-Villanueva, D.; Arenas-García, J. I.; Herrera-Ruiz, D.; Rivera-Islas, J.; Román-Bravo, P.; Morales-Rojas, H.; Höpfl, H. Cocrystals of Active Pharmaceutical Ingredients— Praziquantel in Combination with Oxalic, Malonic, Succinic, Maleic, Fumaric, Glutaric, Adipic, And Pimelic Acids. *Cryst. Growth Des.* **2013**, *13*, 169−185.

(20) Salazar-Rojas, D.; Maggio, R. M.; Kaufman, T. S. Preparation and characterization of a new solid form of praziquantel, an essential anthelmintic drug. Praziquantel racemic monohydrate. *Eur. J. Pharm. Sci.* **2020**, *146*, No. 105267.

(21) Devogelaer, J.-J.; Charpentier, M. D.; Tijink, A.; Dupray, V.; Coquerel, G.; Johnston, K.; Meekes, H.; Tinnemans, P.; Vlieg, E.; ter Horst, J. H.; de Gelder, R. Cocrystals of Praziquantel: Discovery by Network-Based Link Prediction. *Cryst. Growth Des.* **2021**, *21*, 3428−3437.

(22) Borrego-Sánchez, A.; Viseras, C.; Aguzzi, C.; Sainz-Díaz, C. I. Molecular and crystal structure of praziquantel. Spectroscopic properties and crystal polymorphism. *Eur. J. Pharm. Sci.* **2016**, *92*, 266−275.

(23) Zanolla, D.; Perissutti, B.; Vioglio, P. C.; Chierotti, M. R.; Gigli, L.; Demitri, N.; Passerini, N.; Albertini, B.; Franceschinis, E.; Keiser, J.; Voinovich, D. Exploring mechanochemical parameters using a DoE approach: Crystal structure solution from synchrotron XRPD and characterization of a new praziquantel polymorph. *Eur. J. Pharm. Sci.* **2019**, *140*, No. 105084.

(24) Lim, B.-G.; Tan, R. B. H.; Ng, S.-C.; Ching, C.-B. Solubility phase diagram of praziquantel enantiomeric system. *Chirality* **1995**, *7*, 74−81.

(25) Lim, B.-G.; Ching, C.-B.; Tan, R. B. H.; Ng, S.-C. Recovery of (−)-praziquantel from racemic mixtures by continuous chromatography and crystallisation. *Chem. Eng. Sci.* **1995**, *50*, 2289−2298.

(26) Liu, Y.; Wang, X.; Wang, J.-K.; Ching, C. B. Investigation of the phase diagrams of chiral praziquantel. *Chirality* **2006**, *18*, 259−264.

(27) Lorenz, H., Solubility and Solution Equilibria in Crystallization. In *Crystallization: Basic Concepts and Industrial Application*, Beckmann, D. W., Ed. Wiley-VCH: Weinheim, 2013; pp. 35−74.

(28) Lorenz, H.; Sapoundjiev, D.; Seidel-Morgenstern, A. Enantiomeric Mandelic Acid System Melting Point Phase Diagram and Solubility in Water. *J. Chem. Eng. Data* **2002**, *47*, 1280−1284.

(29) Srisanga, S.; ter Horst, J. H. Racemic Compound, Conglomerate, or Solid Solution: Phase Diagram Screening of Chiral Compounds. *Cryst. Growth Des.* **2010**, *10*, 1808−1812.

(30) Kotelnikova, E. N.; Isakov, A. I.; Lorenz, H. Non-equimolar discrete compounds in binary chiral systems of organic substances. *CrystEngComm* **2017**, *19*, 1851−1869.

(31) Huang, J.; Chen, S.; Guzei, I. A.; Yu, L. Discovery of a Solid Solution of Enantiomers in a Racemate-Forming System by Seeding. *J. Am. Chem. Soc.* **2006**, *128*, 11985−11992.

(32) Jacques, J., *Enantiomers, racemates, and resolutions.* Collet, A.; Wilen, S. H., Eds. Wiley: New York:, 1981.

(33) Li, L.; Fijneman, A. J.; Kaandorp, J. A.; Aizenberg, J.; Noorduin, W. L. Directed nucleation and growth by balancing local super-saturation and substrate/nucleus lattice mismatch. *Proc. Natl. Acad. Sci. U. S. A.* **2018**, *115*, 3575.